Experimental and Numerical Study of the Fatigue of GFRP Composites under Complex Loadings

H. Sawadogo[1,2], S. Panier[1,2] and S. Hariri[1,2]

[1] Mines Douai, Polymers and Composites Technology & Mechanical Engineering Dpt, F-59508 Douai, France, E-mail: stephane.panier@mines-douai.fr
[2] Univ Lille Nord de France, F-59000 Lille, France

ABSTRACT. *The behaviour of Glass Fibre Reinforced Polymers (GFRP) laminate composites is studied under static and cyclic in plane complex stress state. The tests were performed on specific cruciform type specimens developed for this study. Several levels of static and cyclic loads were applied to study the fatigue damage evolution and understanding the mutual influence of the stress components. Experimental results show that application of a constant tensile load perpendicularly to a cyclic load has a small influence on the fatigue strength. Finite element simulation is carried out to determine the critically stressed layers and evaluate the ply-by-ply load ratio. It is shown that the critical ply* [±45] *is not influenced by the applied complex loading.*

INTRODUCTION

The most majority of structural composite components experience multi-axial loading during their service life. In spite its importance, the fatigue behaviour of composite materials under complex loading have received only little attention by the scientific community. There are several methods of creating multi-axial loads, including the use of axial forces and pressure (internal/external) using tube specimens, bi-axial plate or cruciform type biaxial configurations and full rig systems applying combinations of axial, bending and/or twisting loads. A recent review on fatigue behavior and life assessment of composite laminate under multiaxial loadings can be found in [1]. Currently, the biaxially loaded cruciform specimen has been identified as of most interest. In addition to test method/standard development, to further increase the confidence of designers, manufacturers and end-users in the use of composite materials for safety critical applications, it is important to be able to apply realistic "service-loading" to components and structures as opposed to just testing simple coupons.

This paper illustrates the preliminary experimental results of a project aimed at investigating the mutual influence of the stress components due to complex loadings on the fatigue behaviour of composite laminates. In this study, tests were performed on specific biaxial cruciform specimens submitted simultaneously to a constant load in one direction and a cyclic tension in the other direction. The influence of the constant load is studied ply-by-ply within finite element simulations.

MATERIAL

The tests were performed on a GFRP made of E-glass/epoxy with a 50% vol. fibre content. Mechanical characterization of the material was made on UD specimens following the classical standards. The average values of elastic and strength properties for the UD tape are summarised in table 1.

Table 1. Mechanical properties of E-glass/epoxy UD

E_L(MPa)	E_T(MPa)	ν_{LT}	G_{LT} (MPa)	X (MPa)	Y (MPa)	S (MPa)
55500	21000	0.29	5500	1100	40	50

L and T indexes are used to indicate respectively the direction along the fibre and transverse direction to the fibre. X is the tensile strength in the direction of the fibres, Y tensile strength transverse to the direction of the fibres and S shear strength in the plane.

Fatigue tests were also performed on UD specimens under tensile load in the direction of the fibres and transverse to the fibres. Shear fatigue behaviour was evaluated by applying tensile load on specimens with [±45°] stacking. All the specimens were tested with a load ratio of 0.1. Five specimens were used for each level. Maximal applied stress is defined as a percentage of the Ultimate Tensile Strength (UTS) given in table 1. Four levels were applied 30%, 45%, 65% and 85% of UTS. SN curves for the different specimens are shown in Figure 1. Classicaly the fatigue strength of UD tape is lower for shear stress than for tensile stress.

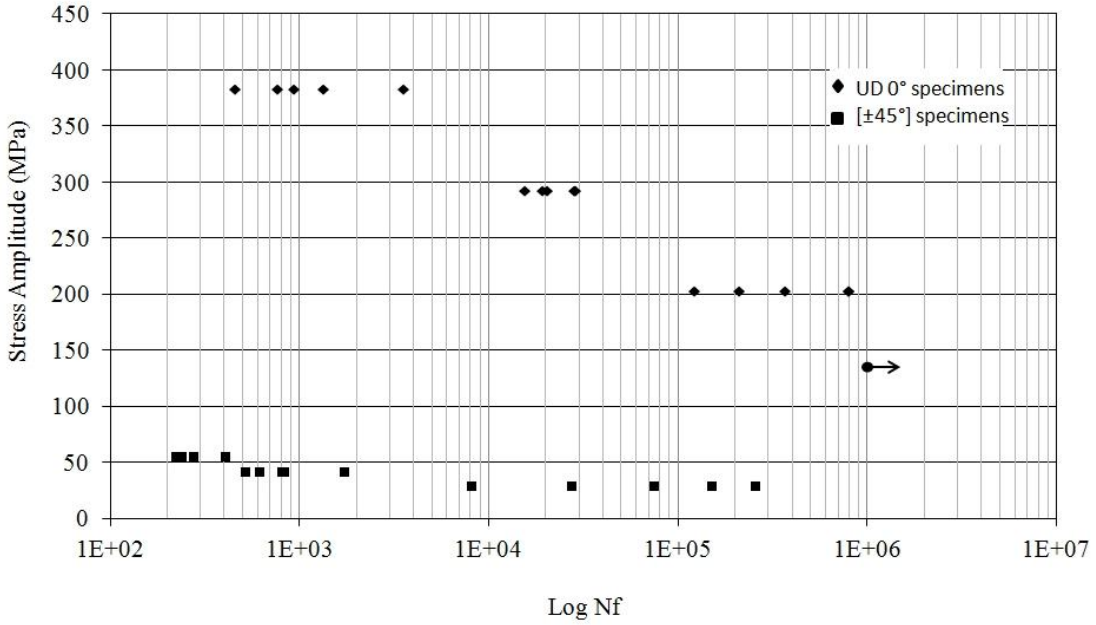

Figure 1: Uniaxial SN curves

EXPERIMENTAL SETUP

Biaxial Test Device

The biaxial tests were carried out on test bench of Institut für Allgemeine Mechanik (IAM) of RWTH Aachen University. The biaxial test rig (Fig. 2) has two actuators with a load capacity of 600 kN for the vertical axis and 150 kN for the horizontal one. The horizontal actuator is mounted in a floating frame to avoid bending moments.

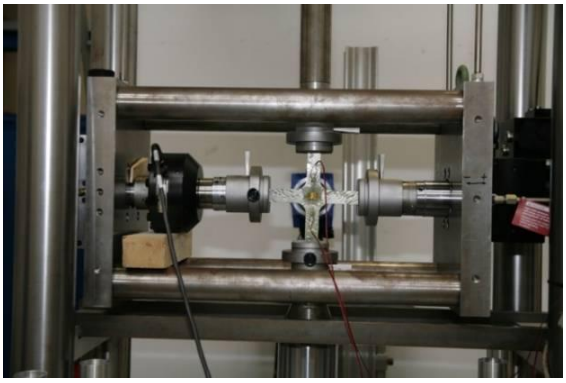

Figure 2: Plane biaxial test device for cruciform specimens

Cruciform Specimen Design

The design and the processing of cruciform specimens for composite laminate are not easy. Different optimized designs have been proposed by several researchers to obtain best and repeatable results by [2-6]. In general, specimens that are suitable for biaxial characterisation must satisfy a number of requirements like maximization of the region of uniform biaxial zone (central gauge section), minimization of the shear strains in the biaxially loaded test zone and final failure should occur within the gauge-section. Finite element simulations were performed on Abaqus to define an optimized geometry (Figure 3) which fulfills the previous requirements.

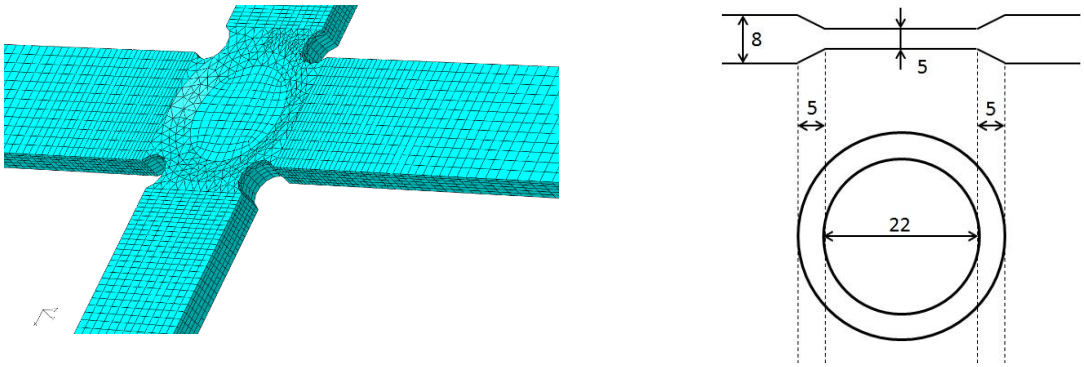

Figure 3:Mesh and details of the optimized cruciform specimen

This design has 25 mm wide arms and a circular gauge section 22 mm in diameter. The specimen width/length was 250 mm. Two different stackings are used: $[0/45/90/-45]_s$ for the central gauge section and $[(\pm 45)_3(0/45/90/-45)]_s$ for the loading arms. The thickness of the central gauge-section was reduced from 8 to 5 mm to promote failure in the gauge section by dropping off three outermost layers over a 5 mm long tapered zone. The corner rounding at the intersection of two perpendicular arms is 4 mm positioned inside the area of the arms to obtain higher strains in the central zone [7].

The calculations were made with the materials data given in table 1. 19500 continuum shell elements were used to define the mesh (Fig. 3). In Figure 5, finite element results for proportional biaxial loading are shown of the first principal strain for the 0° layer (outer ply in the central zone) and +45° layer while in Figure 6 the occurring shear strain is presented. We can observe that the strains in the central zone are uniform. For the 0° layer, the shear strains are zero in the center of the test zone, indicating that the strains measured at the center of the specimen by gauges in the directions of the arms are the principal strains.

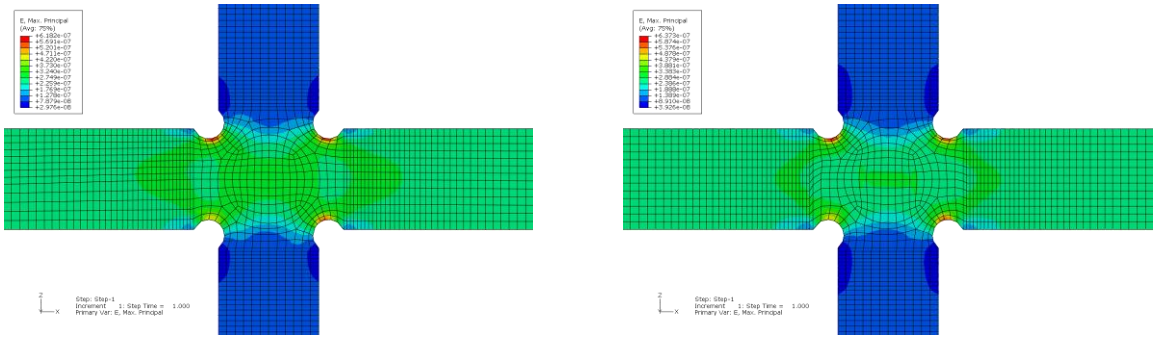

0° PLY 45° PLY

Figure 4: FEM results of the first principal strain in 0° and 45° lay-up

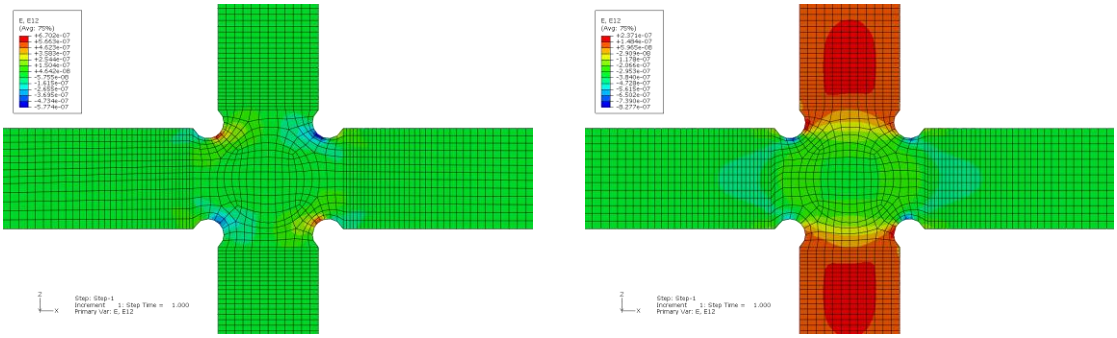

0° PLY 45° PLY

Figure 5: FEM shear strain distributions in 0° and 45° lay-up

EXPERIMENTAL RESULTS

Biaxial tests were performed on cruciform specimens. The applied loading was defined as follow (cf sketch of the figure 6):

- A constant load in the vertical direction with the following levels : 15, 22, 29 and 36% of UTS
- A cyclic loading in the horizontal direction with the following maximal load : 45, 60 and 75% of UTS.

Fatigue tests were carried out at a frequency of 3 Hz and a load ratio of 0.1. The constant applied load is low enough to not damage prematurely the layer oriented at 90° relative to the constant load direction. Three specimens were tested for each level of loading. SN curves obtained are given in Figure 6. Except for the higher cyclic load (75% UTS) we can conclude that application of an additional constant load has a signifiant influence.

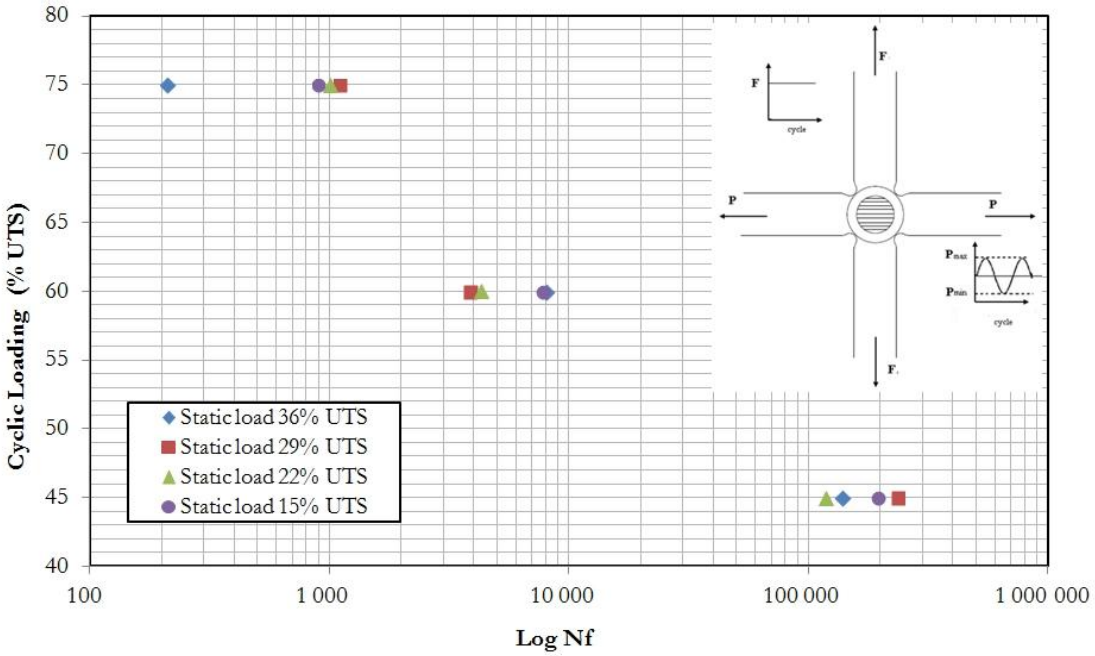

Figure 6: SN curves obtained for different level of constant loads

Stiffness degradations of the specimens under different loadings are given in figure 7. Classicaly stiffness decrease can be divided in three stages. We can remark that constant load have an influence on the stiffness degradation but only during the first stage. In the second stage stiffness evolution has the same slope for the four applied constant load. The first stage of stiffness reduction is due to damages like matrix cracking, fiber/matrix

debonding and transverse cracking. The constant load have an influence on this kind of damages which appear in the layers not parallel to the vertical direction (90° and ±45°).

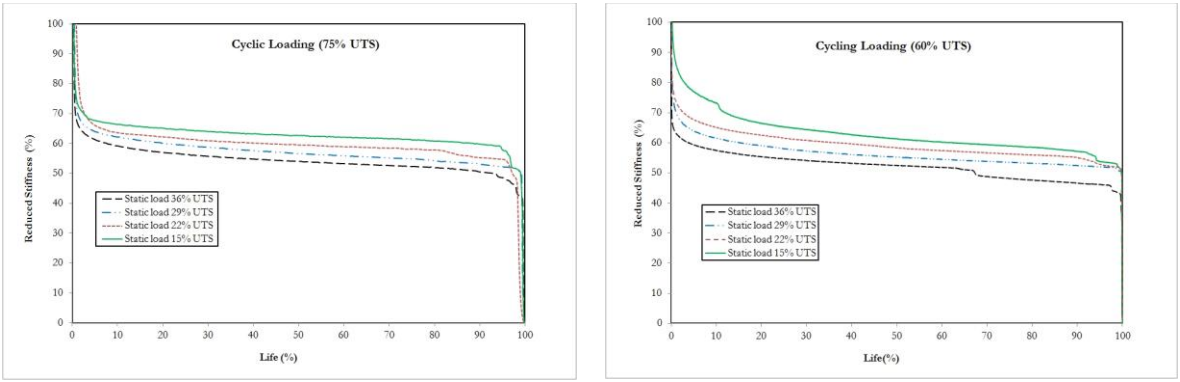

Figure 7: Reduced stiffness in the direction of applied cyclic load during fatigue tests

RESULTS ANALYSIS

Study of the non influence of the static load is done by analysis of the stress state in each ply. Use of failure criterion like Tsai-Hill shows that the critically stressed layer is [±45] one (table 2). For this layer, the influence of the criterion with the value of the constant load F is less sensitive than for the other plies. We can also remark that the critical load is not the same for the different layers: the critical load is P_{max}=45% and F=36% for the plies 0° and 90° and P_{max}=75% and F=36% for the plies [±45].

Table 2. Value of Tsai-Hill criterion in each ply

P_{max}(%)	**75**	**75**	**75**	**75**	**60**	**60**	**60**	**60**	**45**	**45**	**45**	**45**
F (%)	**36**	**29**	**22**	**15**	**36**	**29**	**22**	**15**	**36**	**29**	**22**	**15**
Ply 0	2.7E-2	1.1E-2	9.3E-3	1.2E-2	4.5E-2	1.8E-2	6.0E-3	6.6E-3	7.1E-2	3.3E-2	1.0E-2	3.1E-3
Ply 45	1.0	9.7E-1	9.2E-1	8.8E-1	6.9E-1	6.5E-1	6.1E-1	5.8E-1	4.3E-1	4.0E-1	3.7E-1	3.4E-1
Ply 90	2.4E-3	7.7E-3	3.3E-2	7.6E-2	9.6E-2	2.1E-3	7.3E-3	3.2E-2	3.3E-1	9.6E-2	1.9E-3	7.1E-3

Analysis of the critically stressed ply doesn't give explanation of the non influence of the application of the additional constant load. Here we propose to evaluate the load ratio ply by ply [8]. Due to anisotropic and elastic behaviour of the material, the stress tensor in the ply i can be expressed as the sum of:

- A constant stress tensor $[\sigma_s]_i$ due to the constant load F;
- A constant stress tensor $[\sigma_m]_i$ due to the applied mean cyclic load;

- A time-dependant stress tensor $[\sigma(t)]_i$ due to the variation of the cyclic load.

$$[\sigma]_i = [\sigma_s]_i + [\sigma_m]_i + [\sigma(t)]_i = \begin{bmatrix} \sigma_{11s} & \sigma_{12s} \\ \sigma_{12s} & \sigma_{22s} \end{bmatrix}_i + \begin{bmatrix} \sigma_{11m} & \sigma_{12m} \\ \sigma_{12m} & \sigma_{22m} \end{bmatrix}_i + \begin{bmatrix} \sigma_{11a} & \sigma_{12a} \\ \sigma_{12a} & \sigma_{22a} \end{bmatrix}_i \sin(\omega t) \quad (1)$$

The previous equation can be written as:

$$[\sigma]_i = \begin{bmatrix} \sigma_{11m} + \sigma_{11s} & \sigma_{12m} + \sigma_{12s} \\ \sigma_{12m} + \sigma_{22s} & \sigma_{22m} + \sigma_{22s} \end{bmatrix}_i + \begin{bmatrix} \sigma_{11a} & \sigma_{12a} \\ \sigma_{12a} & \sigma_{22a} \end{bmatrix}_i \sin(\omega t) \quad (2)$$

The global load ratio used for the test is 0.1 which is defined as : $R = \dfrac{\sigma_{ijm} - \sigma_{ija}}{\sigma_{ijm} + \sigma_{ija}} = 0{,}1$

We can define a local load ratio R_{ijL} obtained from the components σ_{ij} of the stress tensor in each ply as:

$$R_{ijL} = \frac{\sigma_{ijm} + \sigma_{ijs} - \sigma_{ija}}{\sigma_{ijm} + \sigma_{ijs} + \sigma_{ija}} \quad (3)$$

The variation of local load ratio is calculated in each ply and each direction from FEM results given by the model presented in the previous section (Table 3) and defined by:

$$\Delta R_{ijL}(\%) = (R_{ijL}(F) - R_{ijL}(F = 36\%)) / R_{ijL}(F = 36\%) * 100 \quad (4)$$

Table 3. Variation of the local load ratios for each ply and each direction calculated for the different applied loads

	F	**29%**	**22%**	**15%**	**29%**	**22%**	**15%**	**29%**	**22%**	**15%**
	P_{max}	**75%**	**75%**	**75%**	**60%**	**60%**	**60%**	**45%**	**45%**	**45%**
Ply 0°	ΔR_{11L}	40	77	110	36	68	96	34	62	86
	ΔR_{22L}	110	-336	-143	40	337	-228	19	76	6037
Ply 90°	ΔR_{11L}	-114	-105	-102	504	-178	-123	48	750	-196
	ΔR_{22L}	-49	-95	-138	-40	-76	-109	-35	-65	-92
Ply +/- 45°	ΔR_{11L}	-11	-22	-36	-10	-22	-36	-10	-21	-35

Directions 1 et 2 are respectively the axis of the vertical and horizontal actuators. As the shear stress in the plies 0° and 90° are very small, the load ratio R_{12L} is not given. For the plies +/- 45°, only one load ratio is reported in the table 3.

We can remark that the level of an applied constant load F perpendicular to a cyclic direction modify the local load ratios of the plies 0° and 90°. But for layer +/- 45°, the variation of the local load ratio is small and proportional. The non influence of the constant load can be explained by the fact that fatigue damage occur first in this lay-up.

CONCLUSION

The results of an experimental investigation on the fatigue behaviour of glass/epoxy cruciform specimens under cyclic tension loading and constant loading has been presented and discussed. Application of an additional constant loading perpendicarly to a cyclic load has no influence on the strength of the specimens. This is explained by the fact that the weakest layer (+/- 45°) is not affected by this additional load. This result can be usefull for the development of new fatigue criteria. Further tests with higher load levels should be performed to confirm these results with higher load levels, on other types of loadings (ex: tubes on axial-torsional loading) and on different stackings like [0/90] for which the influence of an additional constant load is not negligible.

Acknowledgement
Authors gratefully acknowledge the help by Institut für Allgemeine Mechanik (IAM) of RWTH Aachen University for the provivion of the biaxial test facilities.

REFERENCES

1. Quaresimin M.,Susmel L. and Talreja L. (2010) *Int. J. of Fatigue* **32**, 2-16.
2. Welsh, J.S., Adams, D.F. (2002) *Composites Part A* **33**, 829-839.
3. Welsh, J.S., Mayes J.S. and Biskner A.C. (2006) *Composite Structures* **75**, 60-66
4. Smits A., Van Hemelrijck D.V., Philippidis T.P. and Cardon A. (2006) *Composites Science and Technology* **66**, 964-975.
5. Lecompte D., Smits A., Sol H., Vantomme J., Van Hemelrijck D.V. (2007) *Int. J. of Solids and Structures* **44**, 1643-1656.
6. Gower M.R.L., Shaw R.M. (2009) National Physical Laboratory Report MN 09.
7. Lamkanfi E., Van Paepegem W., Degrieck J., Ramault C., Makris A., Van Hemelrijck D.V. (2010) *Polymer Testing* **29**, 7-13.
8. Sawagodo H. (2009). PhD Thesis, University of Lille 1, France.